


Mechanism of Incisional Pain: Novel Finding on Long Noncoding RNA XIST/miR-340-5p/RAB1A Axis

ASN Neuro
Volume 13: 1–14
© The Author(s) 2021
Article reuse guidelines:
sagepub.com/journals-permissions
DOI: 10.1177/17590914211049056
journals.sagepub.com/home/asn


Juan Liao, Fan Zhang, Wenxiang Qing, Rili Yu, and Zhonghua Hu* 

Abstract

The objective of this study is to investigate the effect of long noncoding RNA (lncRNA) XIST on postoperative pain and inflammation of plantar incision pain (PIP) in rats and its underlying mechanisms.

PIP rat models were established by plantar incision. Rats in the sham group were subjected to povidone-iodine scrubbing, and no incision was made. To explore the role of XIST/miR-340-5p/RAB1A in postoperative pain and inflammation, PIP rats were separately or simultaneously injected with lentivirus containing sh-NC, sh-XIST, mimic NC, miR-340-5p mimic, inhibitor NC, miR-340-5p inhibitor, pcDNA3.1, or pcDNA3.1-RAB1A through an intrathecal catheter. The paw withdrawal threshold (PWT) and paw withdrawal latency (PWL) values of rats in each group were assessed to evaluate the pain behavior. RT-qPCR and Western blot were utilized to determine the levels of XIST, miR-340-5p, RAB1A, and NF-κB pathway-related proteins (p-IκBα, IκBα, p-p65, and p65). The concentrations of inflammatory cytokines (TNF-α, IL-1β, and IL-6) in rat spinal dorsal horn tissues were inspected by ELISA. H and E staining was applied to observe the pathological changes of neurons in the spinal dorsal horn, TUNEL staining to detect neuronal apoptosis, and immunohistochemistry to measure RAB1A level.

Plantar incision surgery caused decreased PWT and PWL values, enhanced levels of XIST, RAB1A, and inflammatory cytokines, along with an increased proportion of apoptotic neurons. The pain sensitivity and inflammation of rats were motivated after plantar incision surgery. Intrathecal injection of sh-XIST or miR-340-5p mimic ameliorated the pain and inflammation of PIP rats, while silencing of miR-340-5p or overexpression of RAB1A partly reversed the effect of sh-XIST on PIP rats. XIST targeted miR-340-5p and miR-340-5p negatively regulated RAB1A. The XIST/miR-340-5p/RAB1A axis activated the NF-κB signaling pathway.

LncRNA XIST aggravates inflammatory response and postoperative pain of PIP rats by activating the NF-κB pathway via the miR-340-5p/RAB1A axis.

Keywords

plantar incision pain, XIST, MiR-340-5p, RAB1A, NF-κB pathway, postoperative pain, inflammation

Received May 27, 2021; Revised September 7, 2021; Accepted for publication September 8, 2021

Introduction

Surgery is a first-line therapy choice for many diseases and can lead to numerous complications (Xu et al., 2020). Postoperative pain is a severe acute pain that occurs in patients undergoing a surgery, and there are no adequate analgesics to control the pain (Xu et al., 2019). Although analgesic technologies, such as advanced and multimodal analgesia, have been improving, 39% to 50% of surgical patients still experience moderate to severe acute postoperative pain, which severely affects their recovery (Brennan, 2011). Therefore, investigating the underlying mechanisms of incisional pain and its mediators would facilitate the discovery of novel therapies. Inflammation resulting from surgical injury may contribute to the sensitization of peripheral nociceptors, which may further give rise to hyperalgesia and allodynia (Chen et al., 2018). Furthermore, postoperative pain is proven to be exacerbated by proinflammatory cytokines such as

IL-1β, IL-6, and TNF-α, and these factors are implicated in the hyperalgesia and pain mechanism (Kim et al., 2018). Therefore, further elucidation of the interaction among inflammation, postoperative pain, and plantar incision pain (PIP) is warranted to reveal novel therapeutic targets.

Long noncoding RNA (lncRNA), a class of oligonucleotides longer than 200 nucleotides, bears no protein-coding potentials (Ma et al., 2020; Wang et al., 2020). Increasing

Department of Anesthesiology, the Third Xiangya Hospital, Central South University, Changsha, Hunan 410013, P.R. China

Corresponding Author:

Zhonghua Hu, Department of Anesthesiology, The Third Xiangya Hospital, Central South University, No. 138, Tongzipo Road, Yuelu District, Changsha, Hunan 410013, P.R. China.
E-mail: huzhonghua1983@126.com



Creative Commons Non Commercial CC BY-NC: This article is distributed under the terms of the Creative Commons Attribution-NonCommercial 4.0 License (<https://creativecommons.org/licenses/by-nc/4.0/>) which permits non-commercial use, reproduction and distribution of the work without further permission provided the original work is attributed as specified on the SAGE and Open Access page (<https://us.sagepub.com/en-us/nam/open-access-at-sage>).

evidence indicated that lncRNAs exert crucial functions in gene regulation and biological process, such as inflammation. For example, neuropathic pain and neuroinflammation can be aggravated by lncRNA MALAT1 by regulating the *miR-129-5p*/HMGB1 axis (Ma et al., 2020). X inactive-specific transcript (XIST), located on the long (q) arm of the X chromosome, contributes to neuropathic pain progression in rats (Sun et al., 2018; Wei et al., 2018). More important, XIST is validated to be relative to the inflammatory response of bovine mammary epithelial cells by linking the NF- κ B/NLRP3 inflammasome pathway (Ma et al., 2019). However, the role of XIST in postoperative pain remains poorly elucidated. MicroRNA (miRNA) is a small noncoding RNA of approximately 22 nucleotides that serves as a posttranscriptional regulatory factor of its messenger RNA (mRNA) target (Catalanotto et al., 2016; Xu et al., 2018). Besides, miRNAs are reported to involve in various neuropathological alterations (Peng et al., 2017). A previous study clarified that *miR-340-5p* relieves chronic constriction injury (CCI)-induced neuropathic pain by targeting RAB1A in rat models (Gao et al., 2019). Additionally, excess administration of *miR-340-5p* attenuates the spinal cord injury-induced neuroinflammation of rats (Qian et al., 2020). It is well known that lncRNAs can function as competitive endogenous RNAs (ceRNAs) to modulate disease development by sponging miRNAs and targeting mRNAs (Zhao et al., 2020). Herein, we attempted to identify lncRNA-miRNA-mRNA pair, which might interact with each other, thus affecting postoperative pain. In our current study, we identified *miR-340-5p* as a potential target gene of XIST and an upstream factor of RAB1A. RAB1A is a member of the RAB family (Zhang et al., 2019) and has been previously reported to promote neuroinflammation through activation of the NF- κ B pathway (Song et al., 2020). The *miR-340*/RAB27B axis is actively involved in the occurrence of nonsmall cell lung cancer (Takahashi et al., 2020). In consideration of the potential relationship, we arranged this study to explore the interaction among XIST/*miR-340-5p*/RAB1A, postoperative pain, and inflammatory response in a rat model following plantar incision.

The aim of this study was to examine the regulatory relationship between XIST, *miR-340-5p*, and RAB1A in order to improve the current understanding of the mechanisms underlying postoperative pain. The present study demonstrated that XIST may intensify postoperative pain in PIP rats by activating the NF- κ B pathway via the *miR-340-5p*/RAB1A axis. These findings provided a novel experimental basis for targeted therapy for incisional pain from the aspect of lncRNA-miRNA-mRNA interaction.

Materials and Methods

Ethical Statement

The design of the experiments of this study was approved by the Ethical Committee of Third Xiangya Hospital, Central

South University (No: 2020sydw0630). All experiments in this study were conducted based on the Ethical Guidelines for Animal Experiments of Third Xiangya Hospital, Central South University.

Experimental Animals

Healthy Sprague Dawley (SD) rats were provided by the Shanghai laboratory animal center of the Chinese Academy of Sciences (Shanghai, China), with a total of 50 male rats weighing 193.2 ± 14.6 g. Rats were housed in a laboratory with humidity of $55 \pm 5\%$, and room temperature of $24 \pm 1^\circ\text{C}$ using a 12 h light-dark cycle (light: 6 am ~ 6 pm; dark: 6 pm ~ 6 am) to adapt to the environment for at least one week. Then, they were randomly assigned into ten groups with five rats in each group: Sham, PIP (plantar incision pain), PIP + sh-NC, PIP + sh-XIST, PIP + mimic NC, PIP + *miR-340-5p* mimic, PIP + sh-XIST + inhibitor NC, PIP + sh-XIST + *miR-340-5p* inhibitor, PIP + sh-XIST + pcDNA3.1, and PIP + sh-XIST + pcDNA3.1-RAB1A groups.

Planter Incision

An animal model of postoperative pain was generated by plantar incision as stated in a previous study (Xing et al., 2017). Briefly, rats were anesthetized with 100 mg/kg ketamine and 12 mg/kg xylazine, and the plantar surface of the left hind paw was scrubbed thrice with 10% povidone-iodine. A 1 cm incision was made in the plantar aspect of the left hind paw beginning 0.5 cm from the proximal edge of the heel and extending toward the toes, and skin, fascia, and muscle were incised. The plantaris muscle was isolated, elevated slightly, incised longitudinally, and then put back to its original position. The exposed incision site of the plantaris muscle was desiccated and scrubbed with sterile gauze until hemorrhage was stopped. Then, the skin was opposed with suture using 2-0 nylon. The animals were allowed to return to their home cages after recovering from anesthesia. The incisions were examined daily, and rats with wound infection or dehiscence were excluded from the study. Rats in the sham group were subjected to povidone-iodine scrubbing and no incision was made.

Intrathecal Catheter Implantation and Intrathecal Injection

Animals under ketamine (100 mg/kg) and xylazine (12 mg/kg) anesthesia were implanted with an intrathecal catheter using the method as Yaksh and Rudy described (Yaksh & Rudy, 1976). Briefly, about a 2 cm long midline incision was made in the skin on the midline between the lower margins of both ears (lower margin of occipital prominences), and the subcutaneous tissues were separated to expose the

atlanto-occipital membrane. A 1 ~ 2 mm incision was made on the membrane, and a polyethylene-10 intrathecal catheter (BD, Franklin Lake, NJ) was then placed caudally at approximately 3.3 cm to the T4 spinal cord. The correct intrathecal localization of the catheter was confirmed by the backflow of spinal fluid. The incision was subsequently sutured, with the catheter finally opening cephalic and firmly fixed. The catheter outside of the skin was retained about 3 cm, and the catheter orifice was closed by the application of heat. All rats were fed in single cages after catheterization. To further confirm whether the intrathecal catheter was located in the subarachnoid space of rats, they were monitored for any neurologic deficit (nerve injury or paralysis) on the 7th day after catheterization, and any showing signs of a neurologic deficit were removed from the study.

The intrathecal injection was given once a day, three days before the plantar incision. Rats were separately or simultaneously subjected to ten microliters lentivirus containing sh-NC, sh-XIST, mimic NC, *miR-340-5p* mimic, inhibitor NC, *miR-340-5p* inhibitor, pcDNA3.1, or pcDNA3.1-RAB1A (RiboBio Co., Ltd, Guangzhou, China) (lentivirus titer of 5×10^8 TU/ml) with microsyringe through the intrathecal catheter.

Cell Culture

Human embryonic kidney 293 cells (HEK293 T) were supplied by American Type Culture Collection (ATCC). Cells were immersed in Dulbecco's modified Eagle medium (DMEM, Thermo Fisher Scientific, MA, USA) covering 10% fetal bovine serum and 1% penicillin/streptomycin (Thermo Fisher Scientific) for incubation at 37°C with 5% CO₂.

Behavioral Tests

The rats were tested for paw withdrawal threshold (PWT) and paw withdrawal latency (PWL) before plantar incision, and at days 1, 3, 7, 14, and 21, following the plantar incision. The method was as follows: Rats were placed solely in wire cages for 30 min in a quiet environment. Then, those adapted to the environment and the electronic Von Frey probe (IITC, Woodland Hills, CA, USA) was used to stimulate the soles of their feet three times at an interval of 10 min through the wire cages, and intensity was gradually increased. The pressure values displayed on the Von Frey electronic recorder were recorded when the avoidance reflex occurred in rats, and then the average of the three readings was regarded as the PWT of rats. PWL was regarded as the mean of three readings from the stimulus initiation time to the time of paw retraction in rats. After the pain behavior assessment on the 21st day, the rats were anesthetized with ketamine (100 mg/kg) and xylazine (12 mg/kg), and sacrificed by cervical dislocation. The spinal dorsal horn from L4 to L5 was isolated for follow-up studies.

RT-qPCR

TRIzol (Invitrogen, Carlsbad, CA, USA) was applied to extract the total RNA of the spinal dorsal horn from L4 to L5, and the cDNA template was synthesized by reverse transcription kit. The PCR reaction system was configured by using the fluorescence quantitative PCR kit (Takara, Dalian, China). The RT-qPCR assay was embarked on the ABI7500 real-time PCR instrument (Applied Biosystems, Shanghai, China). Following 10 min of predenaturation at 95°C, cDNA underwent 40 cycles of 10-s denaturing step at 95°C, 20-s annealing step at 60°C, and 34-s extension at 72°C. Subsequently, the expressions of XIST, *miR-340-5p*, and RAB1A were quantitated. The primer sequences are exhibited in **Table 1**. All primers were synthesized by Genewiz Biotechnology Co., Ltd. (Beijing, China). The internal reference of miRNA was U6 and of mRNA was GAPDH, and data analysis utilized the $2^{-\Delta\Delta C_t}$ method (Burja et al., 2019). The formula is as follows: $\Delta\Delta C_t = [C_{t(\text{target gene})} - C_{t(\text{reference gene})}]_{\text{experimental group}} - [C_{t(\text{target gene})} - C_{t(\text{reference gene})}]_{\text{control group}}$.

Western Blot

The tissue homogenate of the spinal dorsal horn in L4-L5 was obtained and washed thrice with precooled phosphate-buffered saline (PBS). Cells were lysed with RIPA cell lysis and subjected to 30 min of standing on ice at 4°C. After 10 min of centrifugation at 12,000 rpm at 4°C, the supernatant was aspirated to 0.5 mL centrifuge tubes for storage under -20°C or protein quantification using a BCA kit (Sigma, MO, USA). The proteins were then exposed to 6×SDS loading buffer at 100°C for denaturation before SDS-PAGE electrophoresis for separation. The proteins were transferred onto membranes using a 4°C precooled transfer buffer for 1.5 h. The membranes were inactivated by 5% non fat dry milk-TBST for 1 h followed by incubation with TBST-diluted primary antibodies against rabbit-derived GAPDH (1:10000, ab181602), RAB1A (1:2000, ab228354), p-IκBα (ab133462, 1:1000), IκBα (ab32518, 1:1000), p-p65 (ab86299, 1:2000), and p65 (ab16502, 1:2000) (Abcam,

Table 1. Primer Sequence Information.

Name of primer	Sequences (5'-3')
LncRNA XIST-F	CAGCCTCGGTCTCTCGAATC
LncRNA XIST-R	CTTGGTGCCAGGATGGAAT
<i>miR-340-5p</i> -F	TTATAAAGCAATGAGACT
<i>miR-340-5p</i> -R	TGGTGTCTGTGGAGTCG
RAB1A-F	AAGCCAGTGAGCTTAGTCCC
RAB1A-R	CGTTGCGTTCTTAGCACTGG
GAPDH-F	ACCACAGTCCATGCCATCAC
GAPDH-R	TCCACCACCCTGTTGCTGTA
U6-F	TCGCTTCGGCAGCACATATAC
U6-R	GCGTGTCTCCTTGCGCAG

Notes: F: forward primer; R: reverse primer.

MA, USA) overnight at 4°C. Before 2 h of incubation with the secondary antibody against goat anti-rabbit IgG or goat anti-mouse IgG (1:5000, Beijing ComWin Biotech Co., Ltd., Beijing, China), the membranes were washed with TBST for 3 × 10 min. The membrane was subjected to color development after another round of TBST washing. After the proteins were incubated with ECL chemiluminescence solution, the membranes were observed under the chemiluminescence imaging analysis system (GE Healthcare, Beijing, China).

ELISA

The levels of TNF- α , IL-1 β , and IL-6 in the spinal dorsal horn from L4 to L5 were determined by ELISA. The tissue homogenate of the spinal dorsal horn was prepared, and the absorbance was measured according to the instructions of the kit (MultiSciences (Lianke) Biotech Co., Ltd., Hangzhou, China). The standard curve was drawn according to the concentration of the standard substance and its absorbance value. The concentration of each sample was calculated according to the optical density (OD) value of the specimen (subtracted from the OD value of the background calibration hole) and the standard curve.

Hematoxylin and Eosin Staining

Rats were anesthetized with ketamine (90 ~ 150 mg/kg) and xylazine (7.5 ~ 16 mg/kg) and then sacrificed by cervical dislocation. The tissues of the spinal dorsal horn in L4-L5 were extracted to prepare 4 μ m paraffin sections. Histopathological changes of spinal cord tissues were observed under the microscope after H and E staining. H and E staining was carried out in strict accordance with the instructions of the H and E staining kit (Beyotime Biotechnology Co., Ltd., Shanghai, China). Briefly, the paraffin sections were deparaffinized by exposure to xylene and then orderly underwent gradient ethanol hydration. Following 5 min of hematoxylin staining, the paraffin sections were subjected to 30 s of differentiation with hydrochloric acid ethanol, 15 min of immersion in tap water, and 3 min of eosin staining. Pictures were captured under a microscope after sections were given dehydration, permeabilization, and seal.

TUNEL Staining

The paraffin sections were dewaxed, hydrated, and permeabilized. Tissues were digested with 20 mg/L proteinase K for 15 min at room temperature and reacted with 500 μ L TUNEL reaction solution (a mixture of 50 μ L TdT solution and 450 μ L fluorescein-labeled dUTP solution) for 1 h at room temperature in a wet box. This process of staining was conducted strictly according to the instructions of the TUNEL kit (In Situ Cell Death Detection Kits, Roche, Indianapolis, IN, USA). Then, cells were incubated with a 50 μ L converter-POD for 30 min and exposed to 100 μ L DAB

substrate for 10 min. After being counterstained with hematoxylin, sections were observed under an optical microscope. The apoptotic rate was calculated. Apoptotic rate = number of apoptotic nucleus / total number of the nucleus.

Immunohistochemistry

Sections were baked for 20 min, dewaxed with conventional xylene, and washed with distilled water. After three times of PBS washing, they were treated with 3% H₂O₂ for 10 min, washed thrice with PBS, and subjected to antigen retrieval, and three times of PBS wash. Then, the sections were blocked with normal goat serum for 20 min. After removal of excess liquid, they were incubated with primary antibody against RAB1A (1:500, ab192446) overnight at 4°C, washed thrice with PBS, and treated with the secondary antibody for 1 h at room temperature. Subsequently, the sections were exposed to DAB for 1-to 3-min color development. This progress was then terminated by three times of PBS washing. Following 3 min of hematoxylin staining, they were dehydrated, permeated, and sealed.

Dual-Luciferase Reporter Assay

The binding site of *miR-340-5p* and lncRNA XIST or RAB1A was predicted by online prediction software StarBase. The mutated and wild-type sequences in the binding sites were designed and cloned into a pmirGLO vector, subsequently renamed as MUT-XIST, WT-XIST, MUT-RAB1A, and WT-RAB1A. Then the vectors were cotransfected with MUT-XIST, WT-XIST, MUT-RAB1A, or WT-RAB1A and *miR-340-5p* mimic (50 nM, GenePharma) or *miR-340-5p* inhibitor (50 nM, GenePharma), respectively, into HEK-239 T cells. Cells were incubated in constant temperature DMEM at 37°C with 5% CO₂ for 48 h, and the fluorescence intensity of cells in each group was assessed by a dual-luciferase reporter kit (Promega, WI, USA).

Statistical Analysis

Statistical analysis of data was performed by SPSS 20.0 (IBM Corp., Armonk, NY, USA) and GraphPad Prism 6.0 (GraphPad Software Inc.). Data were displayed as mean \pm standard deviation (SD). Mann-Whitney *U*-test was adopted for the comparison between two groups. Comparisons among multiple groups were analyzed by Kruskal-Wallis test. *P* < .05 was considered statistically significant.

Results

High Expression of XIST and RAB1A and Low Expression of *miR-340-5p* in PIP Rat Models

PWT and PWL were determined before plantar incision surgery and on days 1, 3, 7, 14, and 21 after surgery, and

the sham group was used as the control group. Compared with the sham group, the PIP group had more sensitive postoperative pain (**Figure 1A-B**, $P < .001$), indicating that PIP models were successfully constructed. Subsequently, analyses of RT-qPCR and Western blot manifested that there were increased expressions of XIST (**Figure 1C**, $P < .001$) and RAB1A (**Figure 1E-F**, $P < .01$), along with a decreased level of *miR-340-5p* (**Figure 1D**, $P < .01$) in the PIP group rather than the sham group. Abnormal expressions of XIST, *miR-340-5p*, and RAB1A suggested that these factors might play crucial roles in postoperative pain.

Results of ELISA addressed the rises in the levels of inflammatory cytokines (IL-6, TNF- α , and IL-1 β) in the spinal dorsal horn of the PIP group (**Figure 1G**, $P < .01$, vs. the sham group). H and E staining results presented that neurons of the spinal dorsal horn in the sham group were characterized by complete structure, orderly arrangement and uniform staining, while neurons in the PIP group were featured by disorderly arrangement, uneven staining, degeneration, and swelling (**Figure 1H**). Additionally, the findings of TUNEL staining illustrated that the number of apoptotic cells was notably increased in the PIP group rather than in the sham group. Many nuclei became pyknotic in round or irregular shapes and then underwent aggregation or fragmentation in the nuclear margin, which is consistent with the morphological changes of apoptotic cells (**Figure 1I**, $P < .01$). The results of immunohistochemistry showed that the expression of RAB1A in spinal dorsal horn neurons of the PIP group was strikingly higher than that in the sham group (**Figure 1J**, $P < .01$). The above results indicated that PIP rat models may have high expressions of XIST and RAB1A as well as low expression of *miR-340-5p*, and pain sensitivity and inflammation may be activated in the PIP rat models.

Inhibition of XIST Ameliorates the Postoperative Pain and Inflammation of PIP Rat Models

To investigate the effect of lncRNA XIST on pain and inflammation in PIP rats, sh-NC or sh-XIST was intrathecally injected into PIP rat models. RT-qPCR detection displayed that the PIP + sh-XIST group possessed lower XIST expression than the PIP + sh-NC group (**Figure 2A**, $P < .01$), showing the good suppressive effect of lncRNA XIST in PIP rats. No significant difference between the PIP group and the PIP + sh-NC group was noted with regard to XIST level (**Figure 2A**). Furthermore, the PWT and PWL of rats were measured on preoperative (day 0), and on postoperative days 1, 3, 7, 14, and 21. We found that compared with the PIP + sh-NC group, the PWT and PWL of the PIP + sh-XIST group were prominently increased, and the postoperative pain was mitigated (**Figure 2B-C**, $P < .01$). ELISA results manifested that intrathecal injection of sh-XIST diminished the levels of IL-1 β and IL-6 and TNF- α in the spinal dorsal horn of the PIP rat models (**Figure 2D**, $P < .01$, PIP + sh-XIST group vs. the PIP +

sh-NC group). The results of H and E staining described that the neurons in PIP + sh-NC group were swollen, disordered, and loose. However, the neurons in the PIP + sh-XIST group was disorderly arranged and the swelling was reduced (**Figure 2E**). Meanwhile, considerable TUNEL-positive cells were found in the PIP + sh-NC group. Nuclei in the PIP + sh-NC group were pyknotic, round or irregular, aggregating into clumps or fragments. There were fewer TUNEL-positive cells in the PIP + sh-XIST group, and the number of apoptotic cells was significantly reduced (**Figure 2F**, $P < .01$). Taken together, suppression of XIST may attenuate the postoperative pain of PIP rat models.

The Pain and Inflammation of PIP Rat Models is Mitigated by miR-340-5p Mimic

PIP rats were given mimic NC or *miR-340-5p* mimic by intrathecal injection to explore the role of *miR-340-5p* in the postoperative pain of PIP rats. Then, the efficiency of *miR-340-5p* mimic was examined by RT-qPCR. We found that intrathecal injection of *miR-340-5p* mimic dramatically elevated *miR-340-5p* level in PIP rats (**Figure 3A**, $P < .001$), while treatment with mimic NC did not alter the expression of *miR-340-5p* (**Figure 3A**). Furthermore, there were increased values of PWT and PWL (**Figure 3B-C**, $P < .01$) and decreased levels of inflammatory cytokines in the PIP + *miR-340-5p* mimic group (**Figure 3D**, $P < .01$, vs. the PIP + mimic NC group) on preoperative (day 0), and on postoperative days 1, 3, 7, 14, and 21. The pathological changes of spinal dorsal horn neurons were detected by H and E staining. The results showed that the PIP + mimic NC group had unevenly stained and swollen neurons in a disorderly arrangement. The neurons in the PIP + *miR-340-5p* mimic group were disorderly arranged; the staining was uniform and neuronal swelling was ameliorated (**Figure 3E**). TUNEL staining was applied to inspect the apoptosis of spinal dorsal horn neurons. The results demonstrated that more TUNEL-positive cells were noticed in the PIP + mimic NC group (**Figure 3F**). Nuclei in the PIP + mimic NC group were pyknotic, round, or irregular aggregating into clumps or fragments. The TUNEL-positive cells in the PIP + *miR-340-5p* mimic group were lowly expressed, and the number of apoptotic cells was diminished (**Figure 3F**, $P < .01$). These results suggested that upregulation of *miR-340-5p* may alleviate inflammation and postoperative pain in PIP rats.

The Negative Relationship Between XIST and miR-340-5p, as well as miR-340-5p and RAB1A

According to the regulatory mechanism of ceRNA, we speculated that XIST may mediate the expression of RAB1A through a miRNA *miR-340-5p*. Subsequently, the StarBase database was employed to predict the relationship between *miR-340-5p* and XIST, as well as *miR-340-5p* and RAB1A.

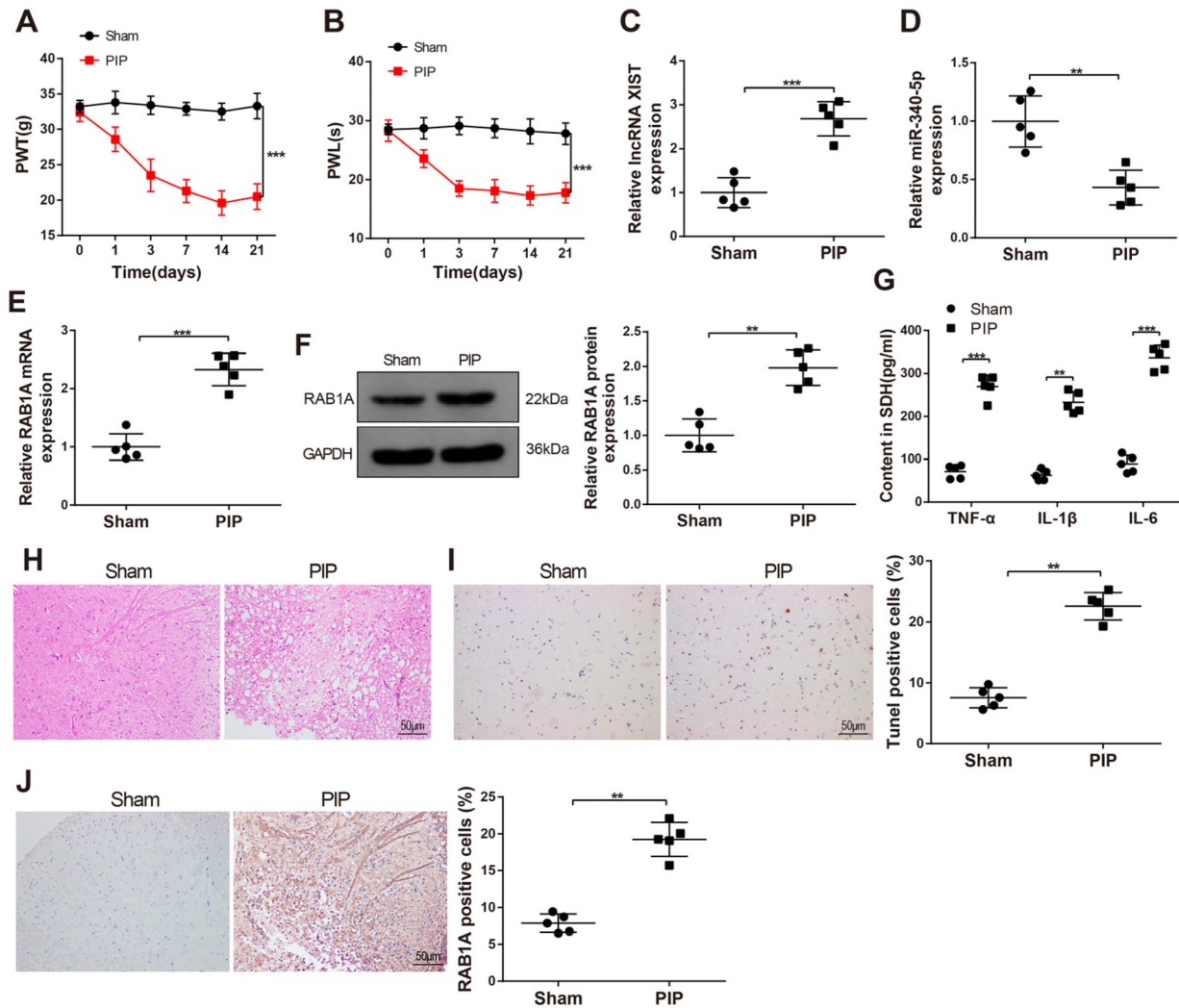


Figure 1. Activated Postoperative Pain Sensitivity and Inflammation in PIP Rat Models

Note. Rat models were established through PIP. On preoperative (day 0), and on postoperative days 1, 3, 7, 14, and 21, the PWT (A) and PWL (B) values were detected. The expression levels of lncRNA XIST (C), *miR-340-5p* (D), and RAB1A (E) in the L4-L5 of the spinal dorsal horn were measured by RT-qPCR, and the protein expression of RAB1A in the L4-L5 of the spinal dorsal horn was inspected by Western blot (F). ELISA was used to determine the concentration of TNF-α, IL-1β, and IL-6 in the spinal dorsal horn tissues of rats (G), and H and E staining to observe the pathological changes of neurons in the spinal dorsal horn (H). The apoptosis of neurons in the spinal dorsal horn was detected by TUNEL staining (I). The expression of RAB1A in the spinal dorsal horn neurons was assessed by immunohistochemistry (J); N = 5. Data were expressed as mean ± standard deviation; ***P* < .01, ****P* < .001, compared with sham group; PIP, plantar incision pain; PWT, paw withdrawal threshold; PWL, paw withdrawal latency.

We found that *miR-340-5p* may be a potential target of XIST, and there was also a binding site of *miR-340-5p* and RAB1A. Therefore, we further speculated that XIST regulates RAB1A by regulating the expression of *miR-340-5p*, thereby playing a crucial role in PIP rats.

To confirm our conjecture, PIP rat models were intrathecally injected with sh-NC, sh-XIST, mimic NC, or *miR-340-5p* mimic. The RT-qPCR results manifested the progressive increase in *miR-340-5p* expression in PIP rats treated with sh-XIST (Figure 4A, *P* < .001, vs. the PIP + mimic NC group), implying that XIST negatively modulated *miR-340-5p* expression. As depicted in Figure 4B, there

were predicted binding and mutation sites of XIST and *miR-340-5p*. To verify the targeting relationship between XIST and *miR-340-5p*, the WT-XIST and MUT-XIST were constructed. Results of dual-luciferase reporter assay displayed that cells cotransfected with WT-XIST and *miR-340-5p* mimic had lower relative luciferase activity than those cotransfected with WT-XIST and mimic NC. Cells cotransfected with WT-XIST and *miR-340-5p* inhibitor had elevated relative luciferase activity than those cotransfected with WT-XIST and inhibitor NC (Figure 4C, *P* < .01). However, the relative luciferase activity of cells cotransfected with MUT-XIST and *miR-340-5p* mimic or *miR-340-5p* inhibitor was not statistically

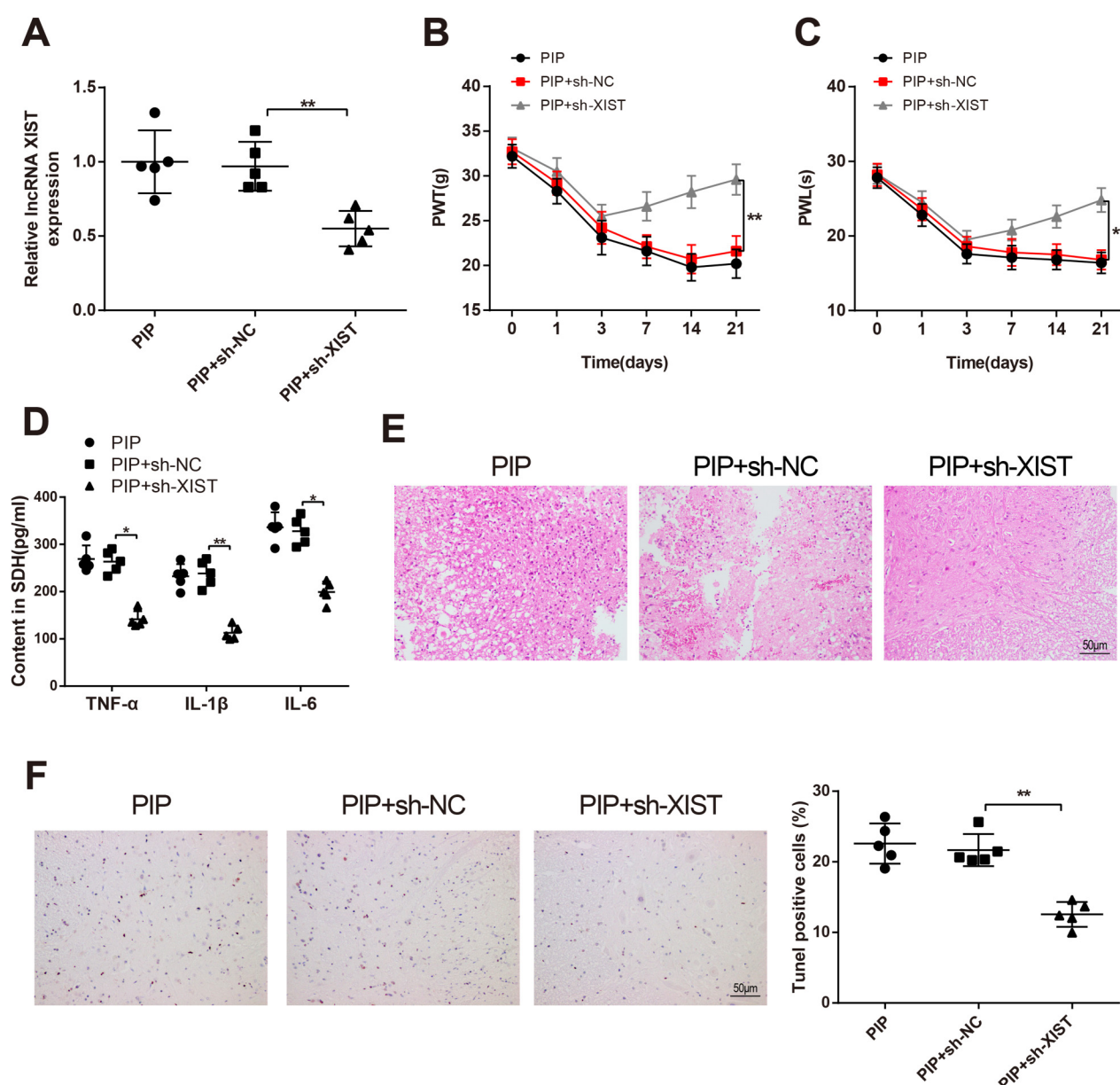


Figure 2. The Postoperative Pain and Inflammatory Response of PIP Rat Models Can be Mitigated by lncRNA XIST

Note. PIP rat models were injected with sh-XIST or sh-NC. Then the mRNA expression level of lncRNA XIST in the L4-L5 of the spinal dorsal horn was examined by RT-qPCR (A). The PWT value (B) and PWL value (C) of rats on preoperative (day 0), and on postoperative days 1, 3, 7, 14, and 21 were calculated. The levels of TNF- α , IL-1 β , and IL-6 were measured by ELISA (D). H and E staining was utilized to observe the pathological changes of neurons in the spinal dorsal horn (E). The apoptosis of neurons in the spinal dorsal horn was assessed by TUNEL staining (F); N = 5. Data were shown as mean \pm standard deviation; * P < .05, ** P < .01, compared with RIP + sh-NC group; PIP, plantar incision pain; PWT, paw withdrawal threshold; PWL, paw withdrawal latency.

different from those cotransfected with MUT-XIST and mimic NC or inhibitor-NC (Figure 4C, P > .05). These findings revealed that XIST may negatively target *miR-340-5p*.

Additionally, the analyses of RT-qPCR and Western blot expounded that the PIP + *miR-340-5p* mimic group had diminished mRNA and protein expressions of RAB1A (Figure 4D-E, P < .01, vs. the PIP + mimic NC group), indicating that RAB1A can be negatively mediated by *miR-340-5p*. Then, the binding site and mutation site of

RAB1A and *miR-340-5p* was predicted by StarBase (Figure 4F). The WT-RAB1A and MUT-RAB1A were accordingly constructed. We found that there were potentiated luciferase activity in cells cotransfected with WT-RAB1A and *miR-340-5p* inhibitor (P < .01, vs. cells cotransfected with WT-RAB1A and inhibitor-NC) and diminished luciferase activity in cells cotransfected with WT-RAB1A and *miR-340-5p* mimic (P < .01, vs. cells cotransfected with WT-RAB1A and mimic-NC). No

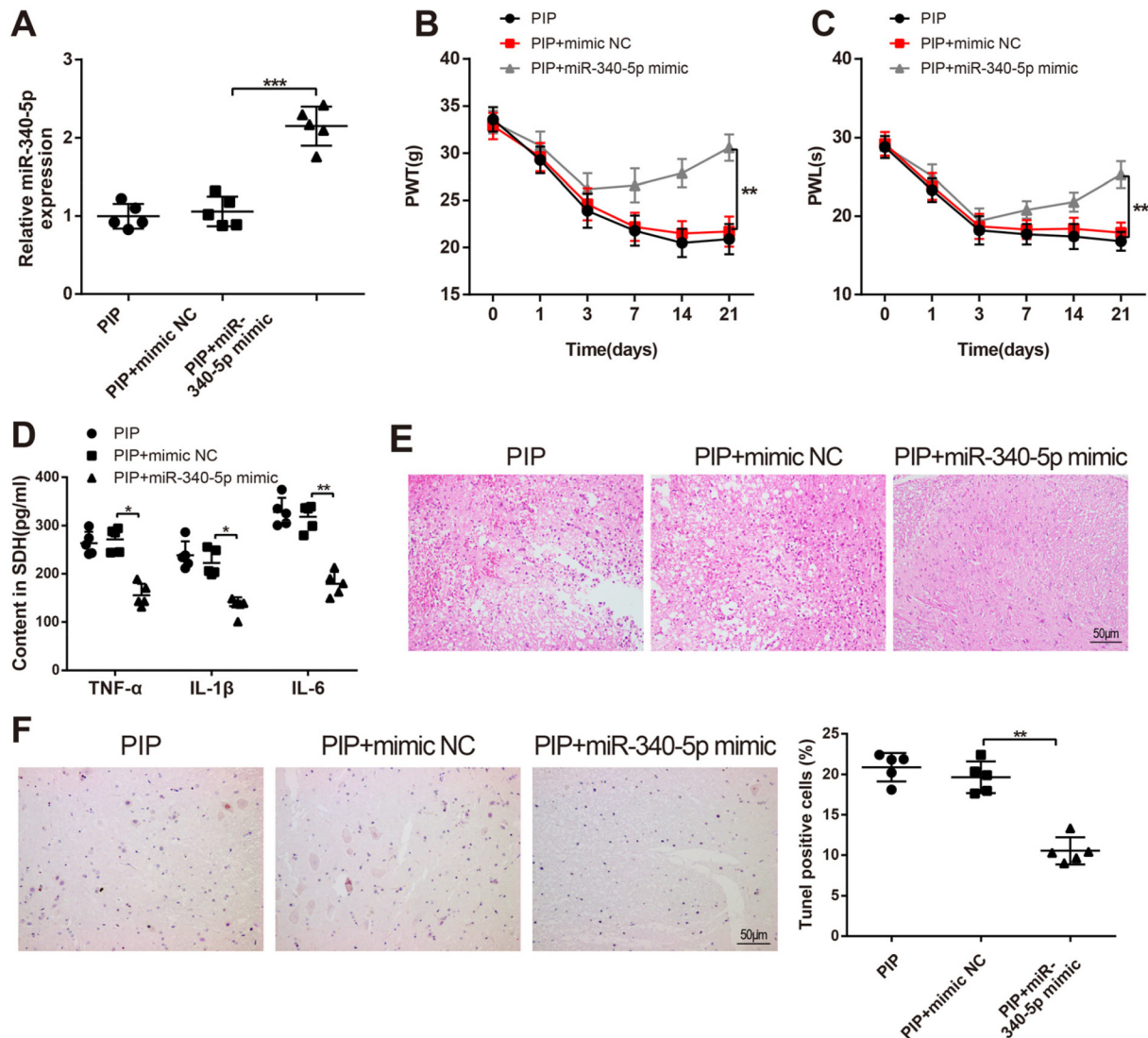


Figure 3. Overexpression of miR-340-5p Relieves the Postoperative Pain and Inflammatory Response of PIP Rat Models

Note. PIP rat models were injected with sh-XIST or sh-NC. RT-qPCR was employed to measure the mRNA expression level of *miR-340-5p* (A) in the L4-L5 of the spinal dorsal horn. The PWT value (B) and PWL value (C) of rats on preoperative (day 0), and on postoperative days 1, 3, 7, 14, and 21 were inspected. The levels of TNF-α, IL-1β, and IL-6 were detected by ELISA (D). The pathological changes of neurons in the spinal dorsal horn were observed after H and E staining (E). The apoptosis of neurons in the spinal dorsal horn was assessed by TUNEL staining (F); N = 5. Data were exhibited as mean ± standard deviation; * $P < .05$, ** $P < .01$, *** $P < .001$, compared with PIP + mimic NC group; PIP, plantar incision pain; PWT, paw withdrawal threshold; PWL, paw withdrawal latency.

notable difference in luciferase activity was observed between cells cotransfected with MUT-RAB1A and *miR-340-5p* mimic or *miR-340-5p* inhibitor and cells cotransfected with MUT-RAB1A and mimic NC or inhibitor-NC (Figure 4G, $P > .05$). The above data illustrated that *miR-340-5p* may negatively target RAB1A.

LncRNA XIST Intensifies the Postoperative Pain of PIP Rat Models via the *miR-340-5p*/RAB1A Axis

To investigate whether XIST could influence PIP rats by regulating the *miR-340-5p*/RAB1A axis, PIP rat models

were solely or simultaneously injected with sh-NC, sh-XIST, inhibitor NC, *miR-340-5p* inhibitor, pcDNA3.1, or pcDNA3.1-RAB1A. The results of RT-qPCR and Western blot exhibited that treatment with sh-XIST decreased the level of RAB1A in PIP rat models ($P < .01$, the PIP + sh-XIST group vs. the PIP + sh-NC group), while the following injection with *miR-340-5p* inhibitor (the PIP + sh-XIST + *miR-340-5p* inhibitor group vs. the PIP + sh-XIST + inhibitor NC group), or pcDNA3.1-RAB1A reinforced RAB1A expression (Figure 5A-B, $P < .05$, the PIP + sh-XIST + pcDNA3.1-RAB1A group vs. the PIP + sh-XIST + pcDNA3.1 group).

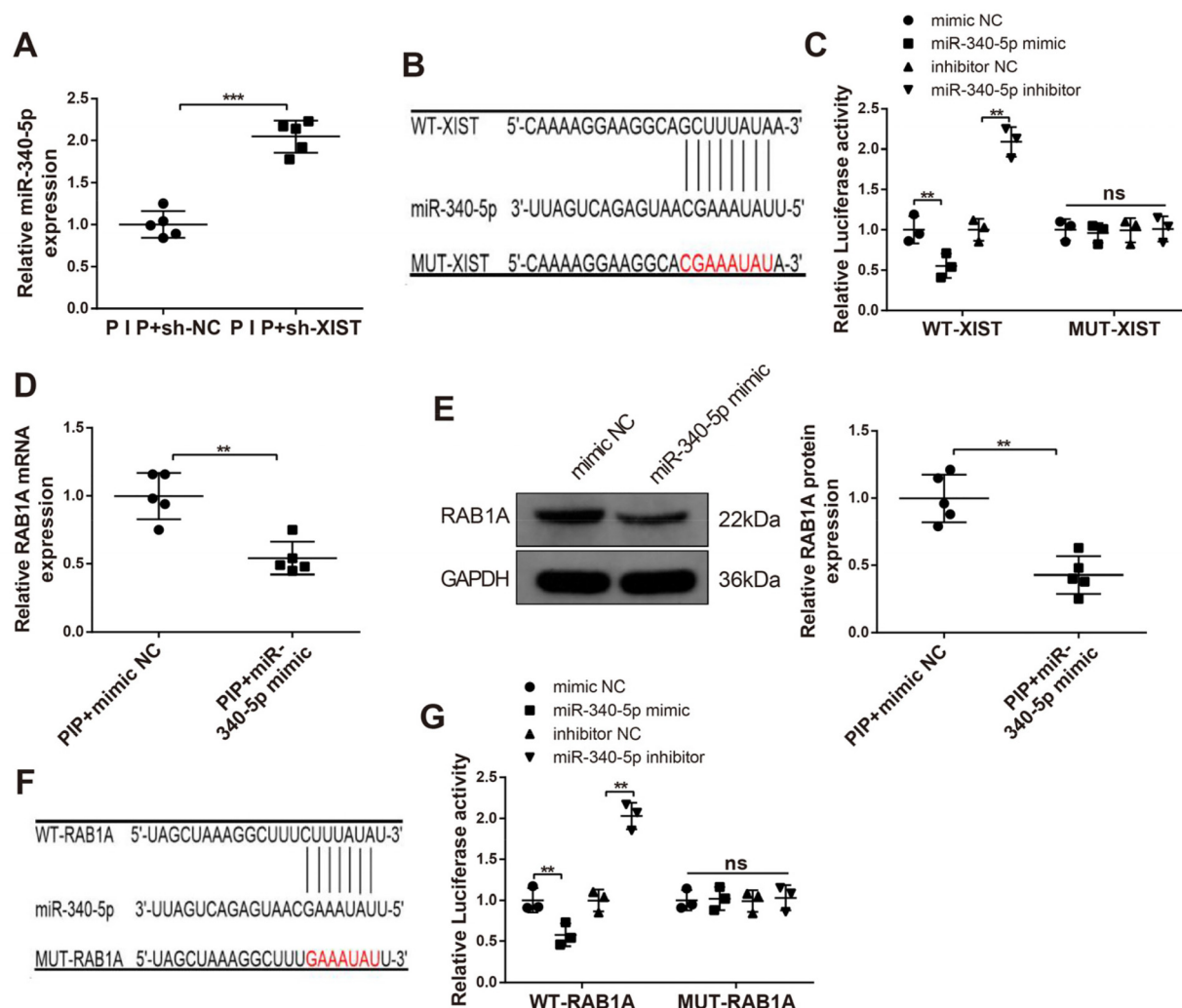


Figure 4. XIST Targets miR-340-5p, and miR-340-5p Negatively Regulates RAB1A

Note. PIP rat models received sh-NC, sh-XIST, mimic NC or *miR-340-5p* mimic by intrathecal injection. Then, RT-qPCR was applied to test the effect of sh-XIST on the expression of *miR-340-5p* in the L4-L5 of the spinal dorsal horn (A), $N = 5$. The binding sites of XIST and *miR-340-5p* were predicted by StarBase, and the mutation sites were accordingly designed (B). Luciferase reporter gene assay was used to measure the relative luciferase activity (C), $N = 3$. PIP rats were injected with mimic NC or *miR-340-5p* mimic, RT-qPCR (D) and Western blot (E) were employed to measure the effect of *miR-340-5p* mimic on RAB1A level in the L4-L5 of the spinal dorsal horn, $N = 5$; The binding sites of RAB1A and *miR-340-5p* were predicted by StarBase, and the mutation sites were accordingly designed (F). Luciferase reporter gene assay was used to measure the relative luciferase activity (G), $N = 3$. Data were expressed as mean \pm standard deviation; ns: not significant; ** $P < .01$, *** $P < .001$, compared with sh-NC or mimic NC group; PIP, plantar incision pain.

In addition, compared with the PIP + sh-NC group, the PIP + sh-XIST group possessed higher values of PWT and PWL (Figure 5C-D, $P < .01$) on preoperative (day 0), and on postoperative days 1, 3, 7, 14, and 21, mitigatory pain and suppressed expressions of inflammatory cytokines (Figure 5E, $P < .01$). However, the PIP + sh-XIST + *miR-340-5p* inhibitor group and PIP + sh-XIST + pcDNA3.1-RAB1A group had reverse trends (Figure 5C-E, $P < .05$, vs. the PIP + sh-XIST + inhibitor NC group or PIP + sh-XIST + pcDNA3.1 group).

H and E staining observed that the neurons in the PIP + sh-NC group were obviously swollen, disordered, and

widely loose. However, the neurons in the PIP + sh-XIST group were disordered, and neuronal swelling was reduced (Figure 5F). Neurons in the PIP + sh-XIST + *miR-340-5p* inhibitor group and the PIP + sh-XIST + pcDNA3.1-RAB1A group appeared to be more swollen and more disorderly arranged than those in the PIP + sh-XIST group (Figure 5F).

TUNEL staining results addressed that more TUNEL-positive cells were noticed in the PIP + sh-NC group (Figure 5G). The karyopyknosis was round or irregular, aggregating into clumps or fragments. In the PIP + sh-XIST group, the TUNEL-positive cells were less and the number of apoptotic cells was reduced (Figure 5G).

However, compared with the PIP + sh-XIST group, increased apoptotic cells were found in the PIP + sh-XIST + *miR-340-5p* inhibitor group and the PIP + sh-XIST + pcDNA3.1-RAB1A group (**Figure 5G**, $P < .05$).

Then, the expression of RAB1A in spinal dorsal horn neurons was measured by immunohistochemistry. The results displayed that injection with sh-XIST repressed the level of RAB1A in PIP rat models ($P < .01$, the PIP + sh-XIST group vs. the PIP + sh-NC group), while the following exposure to *miR-340-5p* inhibitor (the PIP + sh-XIST + *miR-340-5p* inhibitor group vs. the PIP + sh-XIST + inhibitor NC group) or pcDNA3.1-RAB1A heightened RAB1A expression (**Figure 5H**, $P < .05$, the PIP + sh-XIST + pcDNA3.1-RAB1A group vs. the PIP + sh-XIST + pcDNA3.1 group). These findings indicated that the silencing of *miR-340-5p* or overexpression of RAB1A may partly reverse the effect of sh-XIST on PIP rats. The above results suggested that lncRNA XIST may affect the postoperative pain and inflammation of PIP rats via the *miR-340-5p*/RAB1A axis.

XIST Modulates the NF- κ B Signaling Pathway via miR-340-5p/RAB1A Axis

To further study whether NF- κ B could be the downstream signaling pathway of XIST/*miR-340-5p*/RAB1A axis, PIP rats were solely or simultaneously injected with sh-NC, sh-XIST, inhibitor NC, *miR-340-5p* inhibitor, pcDNA3.1, pcDNA3.1-RAB1A, and then the expressions of NF- κ B signaling pathway-related proteins (p-I κ B α , I κ B α , p-p65, and p65) were measured. Western blot presented that rats in the PIP group had higher expressions of p-I κ B α and p-p65 than rats in the sham group ($P < .01$). In addition, intrathecal injection of sh-XIST inhibited the protein levels of NF- κ B pathway-related proteins (**Figure 6**, $P < .01$, PIP + sh-XIST group vs. the PIP + sh-NC group), whereas the following exposure to *miR-340-5p* inhibitor ($P < .05$, the PIP + sh-XIST + *miR-340-5p* inhibitor group vs. the PIP + sh-XIST + inhibitor NC group) or pcDNA3.1-RAB1A (the PIP + sh-XIST + pcDNA3.1-RAB1A group vs. the PIP + sh-XIST + pcDNA3.1 group) enhanced the expressions of p-I κ B α and p-p65 (**Figure 6**, $P < .05$). The above experimental results indicated that suppression of *miR-340-5p* or enhancement of RAB1A may partially reverse the inhibitory effect of sh-XIST on the expressions of p-I κ B α and p-p65. Collectively, the XIST/*miR-340-5p*/RAB1A axis may activate the NF- κ B pathway. The mechanism diagram is showed in **Figure 7**.

Discussion

Patients undergoing surgical operation have clinical postoperative pain even when adjuvant treatments were optimized (Brennan, 2011). Therefore, appropriate postoperative pain

therapy still remains a challenge. The animal model of postoperative pain established by making an incision at the plantar hind paw has similarities to the time course for pain in postoperative patients (Xing et al., 2018). Toward this end, the PIP model in the rat hind paw was used in our study to investigate the role of the XIST/*miR-340-5p*/RAB1A axis in the course of postoperative pain and to identify the novel therapy target.

Postoperative pain is also influenced by an inflammatory response in local injured tissue and the spinal cord (Brennan et al., 1996). In the present study, plantar incision led to enhanced levels of TNF- α , IL-6, and IL-1 β , increased number of apoptotic cells in tissues of the spinal dorsal horn, and decreased values of PWT and PWL. Our data indicated that postoperative pain sensitivity and inflammation may be activated in the PIP rat models. XIST is a lncRNA that mediates the silencing of gene transcription on the X chromosome (Patil et al., 2016). In this study, we analyzed the behavior of lncRNA XIST in the tissues of the spinal dorsal horn. Initially, we observed that PIP rats had higher XIST expression than rats that did not undergo surgery. XIST was therefore speculated to be related to postoperative pain. Subsequently, loss-of-function for XIST proved that deficiency of XIST attenuated the inflammation and postoperative pain of rats following plantar incision. Of note, there has been convincing evidence supporting the role of XIST in neuropathic pain. A study conducted by Yan et al., expounded that XIST can induce neuropathic pain through the upregulation of *miR-150* and ZEB1 (Yan et al., 2018). Downregulation of XIST represses the neuroinflammation of CCI rat models (Jin et al., 2018).

LncRNAs can serve as endogenous RNA and sponge miRNAs to alter their target gene expression at the posttranscriptional level (Chen et al., 2018). As such, we are prompted to further look into the molecular actions of XIST in regulating postoperative pain from the lncRNA-miRNA-mRNA aspect. Herein, we identified *miR-340-5p* as a direct target of XIST by using StarBase software and dual-luciferase reporter assay. Moreover, lowly expressed *miR-340-5p* was found in PIP rats. Results of RT-qPCR addressed that XIST negatively mediated *miR-340-5p* expression in the tissues of the spinal dorsal horn. Toward this end, the potential of *miR-340-5p* in postoperative pain of PIP rats was explored by intrathecal injection of *miR-340-5p* mimic. More interestingly, the findings of behavior test, ELISA, H and E staining, and TUNEL staining demonstrated that the overexpression of *miR-340-5p* relieved the postoperative pain of PIP rats. Consistent with our findings, a previous study also uncovered the performance of *miR-340-5p* in neuropathic pain (Gao et al., 2019). Simultaneously, we found high expression of RAB1A in rats that had undergone plantar incision surgery. RAB proteins modulate membrane transport and impact cell pathways by binding to effector proteins (Li et al., 2017). RAB1A, a member of the RAB family, is closely related to inflammation response (Zhang et al., 2019). In the current

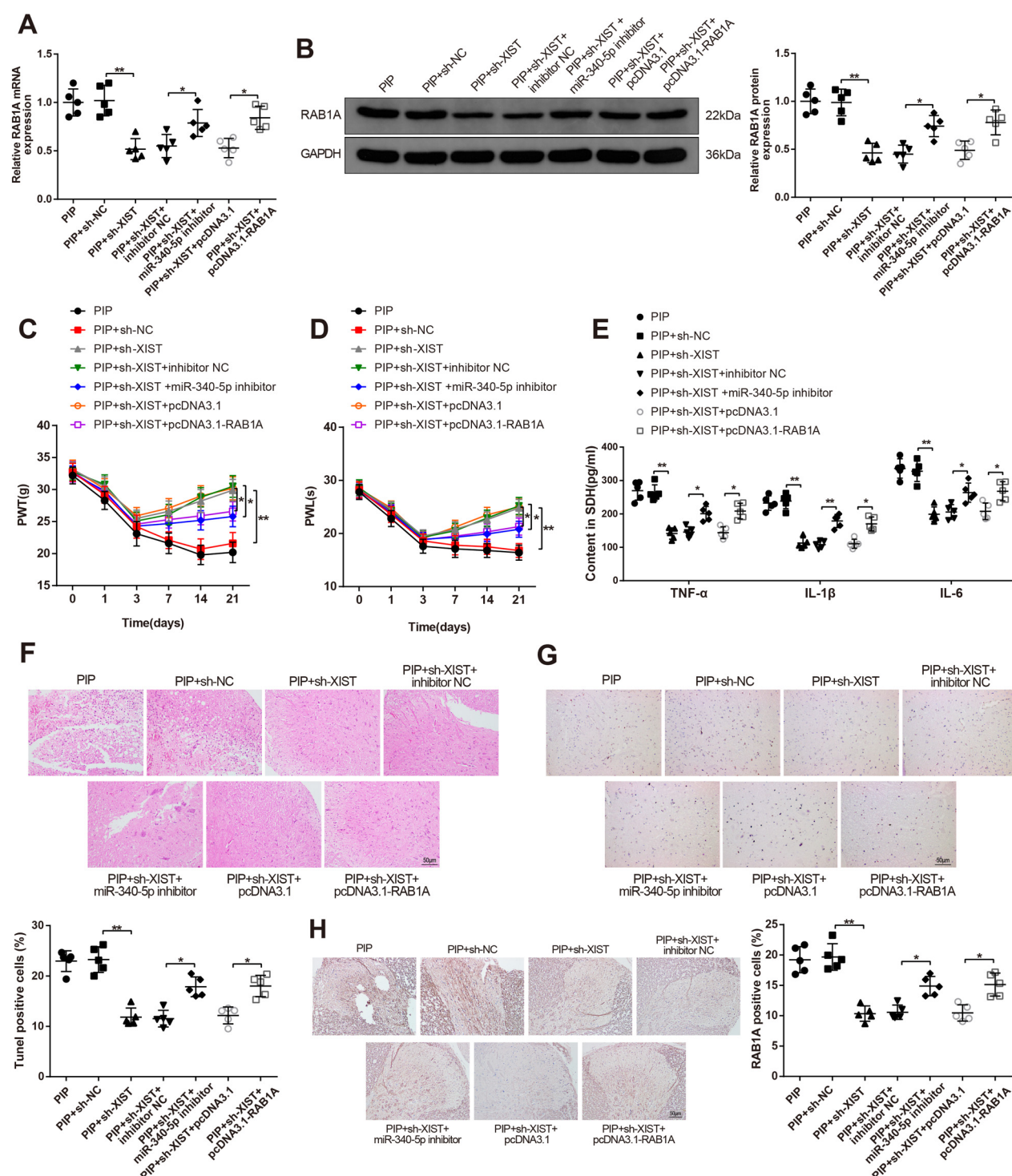


Figure 5. LncRNA XIST Regulates the miR-340-5p/RAB1A Axis to Aggravate the Inflammatory Response and Postoperative Pain of PIP Rat Models

Note. PIP rat models were solely or simultaneously injected with sh-NC, sh-XIST, inhibitor NC, *miR-340-5p* inhibitor, pcDNA3.1, or pcDNA3.1-RAB1A. The mRNA and protein expressions of RAB1A in the L4-L5 of the spinal dorsal horn were detected by RT-qPCR (A) and Western blot (B). The PWT (C) and PWL (D) values on preoperative (day 0), and on postoperative days 1, 3, 7, 14, and 21 were detected before plantar incision surgery and on days 1, 3, 7, 14, and 21 after surgery. ELISA was used to determine the concentrations of TNF- α , IL-1 β , and IL-6 in the spinal dorsal horn tissues of rats (E), and H and E staining to observe the pathological changes of neurons in the spinal dorsal horn (F). The apoptosis of neurons in the spinal dorsal horn was assessed by TUNEL staining (G). The expression of RAB1A in the spinal dorsal horn neurons was detected by immunohistochemistry (H); Data were expressed as mean \pm standard deviation; N = 5; * P < .05, ** P < .01, compared with PIP + sh-NC group, PIP + sh-XIST + inhibitor NC group or PIP + sh-XIST + pcDNA3.1 group; PIP, plantar incision pain; PWT, paw withdrawal threshold; PWL, paw withdrawal latency.

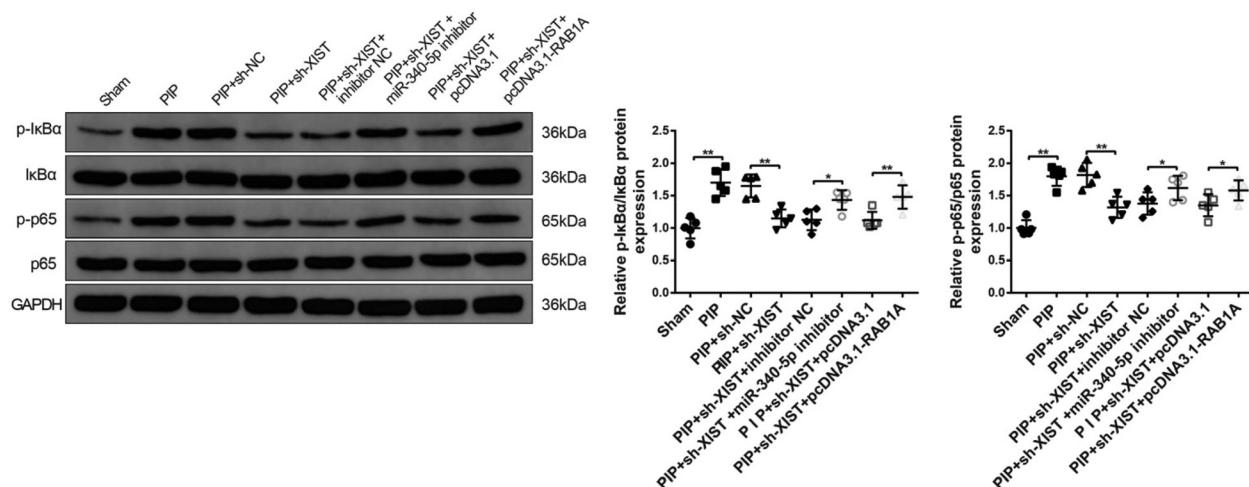


Figure 6. The XIST/*miR-340-5p*/RAB1A Axis Activates the NF- κ B Signaling Pathway

Note. PIP rat models were solely or simultaneously injected with sh-NC, sh-XIST, inhibitor NC, *miR-340-5p* inhibitor, pcDNA3.1, or pcDNA3.1-RAB1A. Western blot was utilized to detect the protein expressions of NF- κ B signaling pathway-related proteins (p-I κ B α , I κ B α , p-p65, and p65) in the L4-L5 of the spinal dorsal horn; N = 5; * P < .05, ** P < .01, compared with sham group, PIP + sh-NC group, PIP + sh-XIST + inhibitor NC group or PIP + sh-XIST + pcDNA3.1 group; PIP, plantar incision pain.

study, the targeting relationship between *miR-340-5p* and RAB1A was also identified. Considering the regulatory mechanism of ceRNA, we speculated that XIST may mediate RAB1A by regulating the expression of *miR-340-5p*, thereby playing a crucial role in PIP rats. Then, our conjecture was confirmed by findings that silencing of *miR-340-5p* or the upregulation of RAB1A partly reversed the role of sh-XIST in PIP rats. Our study proposed that XIST reinforced the pain and inflammation of rats following plantar

incision via the *miR-340-5p*/RAB1A axis. Thus, we provided evidence of the ceRNA-regulatory network in which XIST functioned as a sponge for *miR-340-5p*.

As a key transcriptional factor, NF- κ B is widely expressed in various cells and acts as a key regulator of inflammatory responses (Pei et al., 2018). Activation of NF- κ B begins with the phosphorylation of I κ B α , and once I κ B α is degraded, NF- κ B translocates to the nucleus and facilitates the transcription of its target genes, such as IL-1 β , IL-6, and TNF- α

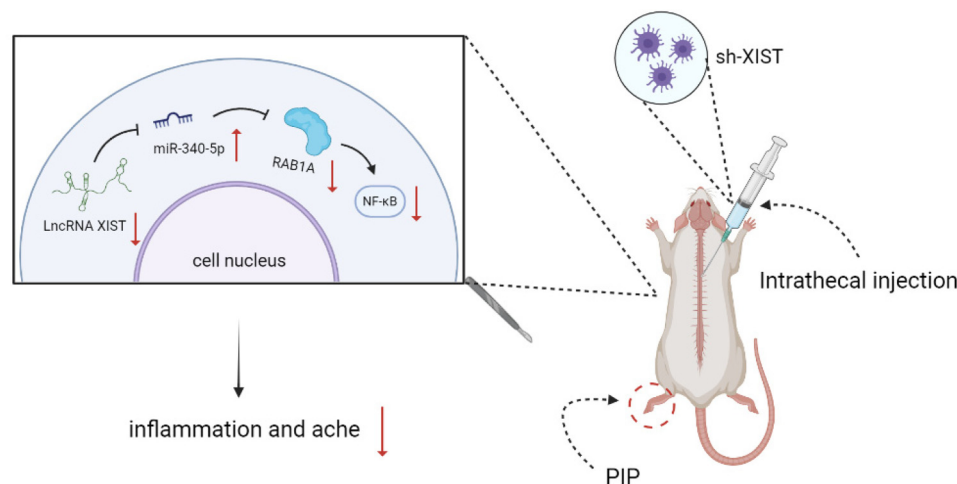


Figure 7. The Mechanism Diagram of LncRNA XIST/*miR-340-5p*/RAB1A Axis Activating NF- κ B Signal Pathway in Enhancing Inflammatory Response and Postoperative Pain of PIP Rat Models

Note. The sh-XIST was injected into the rats in the T4 spinal cord preoperative and for consecutive 3 days before PIP models were established. XIST knockdown suppressed the expression of RAB1A through the LncRNA XIST/*miR-340-5p*/RAB1A axis, which in turn suppressed the NF- κ B signal pathway and attenuated postoperative pain and inflammatory response in PIP rat models. PIP, plantar incision pain.

(Fuentes et al., 2016; Schuster et al., 2013). Toward this end, the NF- κ B pathway was selected and the protein expressions of NF- κ B signaling pathway-related proteins were measured in our study. We revealed that NF- κ B was the downstream pathway of the XIST/*miR-340-5p*/RAB1A axis. A former study expounded that NF- κ B can control the expressions of proinflammatory and pain mediators (Liang et al., 2017). Additionally, the NF- κ B pathway plays an indispensable role in inflammatory response modulated by lncRNA XIST (Ma et al., 2019). Here, we further proposed that lncRNA XIST activated the NF- κ B pathway via the *miR-340-5p*/RAB1A axis to intensify postoperative pain and the inflammatory response of PIP rats.

There are two limitations of this study that we should bear in mind. Currently, pain research has greatly relied on animal models to understand mechanisms and to advance new therapies. However, due to the differences between rodents and humans, it is often difficult to come to clear conclusions. In addition, even within the species, pain-related behaviors are also influenced by variables such as sex and the nociceptive test used. Therefore, more researches and verifications on the result of this study are still needed. These limitations are inevitable in a study, but it also provides potential directions for our future studies.

In summary, we report the roles of XIST in rats after plantar incision surgery. Our findings elucidate that XIST reinforces pain and inflammation of PIP rats, by functioning as a ceRNA for *miR-340-5p*, and subsequently, activating the NF- κ B pathway; thus emphasizing the potentials of the XIST/*miR-340-5p*/RAB1A axis in the therapy for postoperative pain.

Acknowledgments

Thanks to all the contributors.


Conflict of Interests

The authors declare there is no conflict of interest.

Funding

This study was funded by the grant from the National Natural Science Foundation of China (Grant No. 81571879).

ORCID iD

Zhonghua Hu  <https://orcid.org/0000-0001-7979-1279>

References

- Brennan, T. J. (2011). Pathophysiology of postoperative pain. *Pain*, 152(3 Suppl), S33–S40.
- Brennan, T. J., Vandermeulen, E. P., & Gebhart, G. F. (1996). Characterization of a rat model of incisional pain. *Pain*, 64(3), 493–502.
- Burja, B., Kuret, T., Janko, T., Topalovic, D., Zivkovic, L., Mrak-Poljsak, K., Spremo-Potparevic, B., Zigon, P., Distler, O., Cucnik, S., Sodin-Semrl, S., Lakota, K., & Frank-Bertoncelj, M. (2019). Olive leaf extract attenuates inflammatory activation and DNA damage in human arterial endothelial cells. *Frontiers in Cardiovascular Medicine*, 6, 56.
- Catalanotto, C., Cogoni, C., & Zardo, G. (2016). MicroRNA in control of gene expression: An overview of nuclear functions. *International Journal of Molecular Sciences*, 17(10).
- Chen, X., Zeng, K., Xu, M., Hu, X., Liu, X., Xu, T., He, B., Pan, Y., Sun, H., & Wang, S. (2018a). SP1-induced lncRNA-ZFAS1 contributes to colorectal cancer progression via the miR-150-5p/VEGFA axis. *Cell Death & Disease*, 9(10), 982.
- Chen, X., Zhang, B., Li, J., Feng, M., Zhang, Y., Yao, W., Zhang, C., & Wan, L. (2018b). Celastrol attenuates incision-induced inflammation and pain associated with inhibition of the NF-kappaB signalling pathway via SARM. *Life Sciences*, 205, 136–144.
- Fuentes, E., Rojas, A., & Palomo, I. (2016). NF-kappaB signaling pathway as target for antiplatelet activity. *Blood Reviews*, 30(4), 309–315.
- Gao, L., Pu, X., Huang, Y., & Huang, J. (2019). MicroRNA-340-5p relieved chronic constriction injury-induced neuropathic pain by targeting Rap1A in rat model. *Genes & Genomics*, 41(6), 713–721.
- Jin, H., Du, X. J., Zhao, Y., & Xia, D. L. (2018). XIST/miR-544 axis induces neuropathic pain by activating STAT3 in a rat model. *Journal of Cellular Physiology*, 233(8), 5847–5855.
- Kim, M. K., Kang, H., Baek, C. W., Jung, Y. H., Woo, Y. C., Choi, G. J., Shin, H. Y., & Kim, K. S. (2018). Antinociceptive and anti-inflammatory effects of ginsenoside Rf in a rat model of incisional pain. *Journal of Ginseng Research*, 42(2), 183–191.
- Li, Y., Xia, H., Chen, L., & Zhang, X. (2017). Sevoflurane induces endoplasmic reticulum stress mediated apoptosis in mouse hippocampal neuronal HT22 cells via modulating miR-15b-5p/Rab1A signaling pathway. *International Journal of Clinical and Experimental Pathology*, 10(8), 8270–8280.
- Liang, F., Liu, M., Fu, X., Zhou, X., Chen, P., & Han, F. (2017). Dexmedetomidine attenuates neuropathic pain in chronic constriction injury by suppressing NR2B, NF-kappaB, and iNOS activation. *Saudi Pharmaceutical Journal*, 25(4), 649–654.
- Ma, M., Pei, Y., Wang, X., Feng, J., Zhang, Y., & Gao, M. Q. (2019). lncRNA XIST mediates bovine mammary epithelial cell inflammatory response via NF-kappaB/NLRP3 inflammatory pathway. *Cell Proliferation*, 52(1), e12525.
- Ma, X., Wang, H., Song, T., Wang, W., & Zhang, Z. (2020). lncRNA MALAT1 contributes to neuropathic pain development through regulating miR-129-5p/HMGB1 axis in a rat model of chronic constriction injury. *The International Journal of Neuroscience*, 130(12), 1215–1224.
- Patil, D. P., Chen, C. K., Pickering, B. F., Chow, A., Jackson, C., Guttman, M., & Jaffrey, S. R. (2016). M(6)A RNA methylation promotes XIST-mediated transcriptional repression. *Nature*, 537(7620), 369–373.
- Pei, W., Zou, Y., Wang, W., Wei, L., Zhao, Y., & Li, L. (2018). Tizanidine exerts anti-nociceptive effects in spared nerve injury model of neuropathic pain through inhibition of TLR4/NF-kappaB pathway. *International Journal of Molecular Medicine*, 42(6), 3209–3219.
- Peng, C., Li, L., Zhang, M. D., Bengtsson Gonzales, C., Parisien, M., Belfer, I., Usoskin, D., Abdo, H., Furlan, A., Haring, M., Lallemand, F., Harkany, T., Diatchenko, L., Hokfelt, T., Hjerling-Leffler, J., & Ernfors, P. (2017). miR-183 cluster scales mechanical pain sensitivity by regulating basal and

- neuropathic pain genes. *Science (New York, N Y)*, 356(6343), 1168–1171.
- Qian, Z., Chang, J., Jiang, F., Ge, D., Yang, L., Li, Y., Chen, H., & Cao, X. (2020). Excess administration of miR-340-5p ameliorates spinal cord injury-induced neuroinflammation and apoptosis by modulating the P38-MAPK signaling pathway. *Brain Behavior and Immunity*, 87, 531–542.
- Schuster, M., Annemann, M., Plaza-Sirvent, C., & Schmitz, I. (2013). Atypical IkappaB proteins - nuclear modulators of NF-kappaB signaling. *Cell Communication and Signaling*, 11(1), 23.
- Song, S., Pan, Y., Li, H., & Zhen, H. (2020). MiR-1202 exerts neuroprotective effects on OGD/R induced inflammation in HM cell by negatively regulating Rab1a involved in TLR4/NF-kappaB signaling pathway. *Neurochemical Research*, 45(5), 1120–1129.
- Sun, W., Ma, M., Yu, H., & Yu, H. (2018). Inhibition of lncRNA X inactivate-specific transcript ameliorates inflammatory pain by suppressing satellite glial cell activation and inflammation by acting as a sponge of miR-146a to inhibit Nav 1.7. *Journal of Cellular Biochemistry*, 119(12), 9888–9898.
- Takahashi, K., Koyama, K., Ota, Y., Iwamoto, H., Yamakita, K., Fujii, S., & Kitano, Y. (2020). The interaction between long Non-coding RNA HULC and MicroRNA-622 via transfer by extracellular vesicles regulates cell invasion and migration in human pancreatic cancer. *Frontiers in Oncology*, 10, 1013.
- Wang, L., Luo, Y., Zheng, Y., Zheng, L., Lin, W., Chen, Z., Wu, S., Chen, J., & Xie, Y. (2020). Long non-coding RNA LINC00426 contributes to doxorubicin resistance by sponging miR-4319 in osteosarcoma. *Biology Direct*, 15(1), 11.
- Wei, M., Li, L., Zhang, Y., Zhang, Z. J., Liu, H. L., & Bao, H. G. (2018). LncRNA X inactive specific transcript contributes to neuropathic pain development by sponging miR-154-5p via inducing toll-like receptor 5 in CCI rat models. *Journal of Cellular Biochemistry*.
- Xing, F., Kong, C., Bai, L., Qian, J., Yuan, J., Li, Z., Zhang, W., & Xu, J. T. (2017). CXCL12/CXCR4 Signaling mediated ERK1/2 activation in spinal cord contributes to the pathogenesis of post-surgical pain in rats. *Molecular Pain*, 13, 1744806917718753.
- Xing, F., Zhang, W., Wen, J., Bai, L., Gu, H., Li, Z., Zhang, J., Tao, Y. X., & Xu, J. T. (2018). TLR4/NF-kappaB Signaling activation in plantar tissue and dorsal root ganglion involves in the development of postoperative pain. *Molecular Pain*, 14, 1744806918807050.
- Xu, B., Liu, S. S., Wei, J., Jiao, Z. Y., Mo, C., Lv, C. M., Huang, A. L., Chen, Q. B., Ma, L., & Guan, X. H. (2020). Role of spinal cord Akt-mTOR signaling pathways in postoperative hyperalgesia induced by plantar incision in mice. *Frontiers in Neuroscience*, 14, 766.
- Xu, B., Mo, C., Lv, C., Liu, S., Li, J., Chen, J., Wei, Y., An, H., Ma, L., & Guan, X. (2019). Post-surgical inhibition of phosphatidylinositol 3-kinase attenuates the plantar incision-induced postoperative pain behavior via spinal Akt activation in male mice. *BMC Neuroscience*, 20(1), 36.
- Xu, J., Pan, X., & Hu, Z. (2018). MiR-502 mediates esophageal cancer cell TE1 proliferation by promoting AKT phosphorylation. *Biochemical and Biophysical Research Communications*, 501(1), 119–123.
- Yaksh, T. L., & Rudy, T. A. (1976). Chronic catheterization of the spinal subarachnoid space. *Physiology & Behavior*, 17(6), 1031–1036.
- Yan, X. T., Lu, J. M., Wang, Y., Cheng, X. L., He, X. H., Zheng, W. Z., Chen, H., & Wang, Y. L. (2018). XIST Accelerates neuropathic pain progression through regulation of miR-150 and ZEB1 in CCI rat models. *Journal of Cellular Physiology*, 233(8), 6098–6106.
- Zhang, Y., Wang, L., Lv, Y., Jiang, C., Wu, G., Dull, R. O., Minshall, R. D., Malik, A. B., & Hu, G. (2019). The GTPase Rab1 Is required for NLRP3 inflammasome activation and inflammatory lung injury. *Journal of Immunology*, 202(1), 194–206.
- Zhao, S., Xiong, W., & Xu, K. (2020). MiR-663a, regulated by lncRNA GAS5, contributes to osteosarcoma development through targeting MYL9. *Human & Experimental Toxicology*, 39(12), 1607–1618.